Science Advances
AAAS

Supplementary Materials for

Conserved conformational dynamics determine enzyme activity

Kristiane R. Torgeson *et al.*

Corresponding author: Wolfgang Peti, peti@uchc.edu

Sci. Adv. **8**, eabo5546 (2022)
DOI: 10.1126/sciadv.abo5546

This PDF file includes:

Table S1: Enzymatic activity (Michaelis-Menten analysis) and protein stability (T_M)

Variant	k_{cat} (s^{-1})	f	K_M (μM)	f	k_{cat} / K_M (s^{-1}μM^{-1})	f	R^2	N	ΔT_m(°C)
PTP1B	11.4 ± 0.9	--	496.1 ± 26.2	--	23.1 ± 3.7	--	0.990	13	(57.7)
$PTP1B_{F225I}$	6.8 ± 0.3	0.6	688.3 ± 38.3	1.4	9.9 ± 0.7	0.4	0.958	3	-11.6
$PTP1B_{F225L}$	7.6 ± 0.3	0.7	660.0 ± 44.5	1.4	11.5 ± 0.9	0.5	0.962	3	-7.9
$PTP1B_{F225Y}$	20.3 ± 0.9	1.8	600.8 ± 36.2	1.2	33.7 ± 2.5	1.5	0.974	4	-7.7
$PTP1B_{R199N}$	11.0 ± 0.5	1.0	530.7 ± 30.9	1.6	20.7 ± 1.6	0.9	0.985	3	-6.0
$PTP1B_{FYRN}$	25.1 ± 1.1	2.2	655.0 ± 30.7	1.3	38.3 ± 2.4	1.7	0.985	3	-10.0
$PTP1B_{RNLR}$	36.2 ± 1.7	3.2	868.8 ± 27.5	1.8	41.6 ± 2.3	1.8	0.995	4	-8.5
$PTP1B_{FYRNLR}$	45.0 ± 1.9	3.9	598.0 ± 25.7	1.2	75.3 ± 4.6	3.3	0.984	3	-10.6
$PTP1B_{L204A}$	23.6 ± 1.0	2.1	505.7 ± 20.4	1.1	46.7 ± 2.7	2	0.990	4	-5.5
$PTP1B_{P206G}$	12.0 ± 0.6	1.1	551.1 ± 41.4	1.1	21.7 ± 1.9	0.9	0.952	3	-2.8
$PTP1B_{GGGGG}$	21.6 ± 1.0	1.9	839.8 ± 26.1	1.7	25.7 ± 1.4	1.1	0.995	3	-11.6
PTP1BΔ7	8.6 ± 0.2	--	900.6 ± 30.0	--	9.6 ± 0.4	--	0.989	4	(54.9)
$PTP1B\Delta7_{F225Y}$	16.1 ± 0.5	1.9	987.9 ± 25.0	1.1	16.3 ± 0.6	1.7	0.994	4	-6.8
$PTP1B\Delta7_{FYRN}$	18.0 ± 0.2	2.1	1054.4 ± 42.2	1.2	17.0 ± 0.7	1.8	0.987	4	-8.3
$PTP1B\Delta7_{FYRNLR}$	40.60 ± 1.0	4.7	843.9 ± 25.1	0.9	48.1 ± 1.8	5.0	0.992	4	-9.3

Table S2: Data Collection and Statistics of PTP1B Variant Crystal Structures

	PTP1B F225Y	PTP1B F225Y + TCS401	PTP1BΔ7 FYRN	PTP1BΔ7 FYRN + TCS401	PTP1BΔ7 FYRNLR	PTP1B FYRNLR + TCS401	PTP1B L204A	PTP1B L204A + TCS401
PDB	7MKZ	7MN7	7MN9	7MNA	7MOU	7MNB	7MNC	7MND
Data Collection								
Beamline	SSRL 12-2	SSRL 12-2	SSRL 12-2	SSRL 12-2	SSRL 12-2	SSRL 12-2	SSRL 12-2	SSRL 12-2
Space group	P 3_2 2 1	P 3_1 2 1	P 3_2 2 1	P 3_2 2 1	P 3_2 2 1	P 3_1 2 1	P 3_2 2 1	P 3_1 2 1
Unit cell	88.6 88.6 72.6 90 90 120	88.5 88.5 104.2 90 90 120	88.5 88.5 72.4 90 90 120	88.0 88.0 72.3 90 90 120	88.4 88.4 72.5 90 90 120	88.8 88.8 106.0 90 90 120	87.6 87.6 71.1 90 90 120	88.3 88.3 105.0 90 90 120
Resolution (Å)	37.81 - 1.40 (1.42 - 1.40)	38.33 - 1.95 (2.00 - 1.95)	38.31 - 1.24 (1.26 - 1.24)	38.11 - 1.47 (1.49 - 1.47)	38.29 - 1.48 (1.50 - 1.48)	38.46 - 2.2 (2.27 - 2.2)	37.97 - 1.85 (1.89 - 1.85)	21.64 - 2.29 (2.37 - 2.29)
Multiplicity	10.0 (9.4)	11.3 (10.9)	8.1 (7.0)	3.7 (3.4)	11.1 (10.2)	11.1 (11.0)	11.2 (10.2)	6.5 (1.7)
Completeness (%)	99.6 (96.0)	99.7 (98.8)	99.5 (92.1)	98.9 (96.0)	99.8 (98.1)	98.5 (98.8)	97.6 (85.8)	99.3 (98.7)
I/sigma(I)	14.6 (1.5)	15.5 (1.9)	15.9 (1.6)	14.7 (2.42)	19.2 (2.2)	13.0 (2.4)	17.1 (4.8)	12.8 (2.3)
R-merge	0.076 (1.40)	0.115 (1.305)	0.056 (0.607)	0.045 (0.525)	0.073 (1.047)	0.138 (1.032)	0.087 (0.605)	0.0223 (0.341)
CC1/2	1.00 (0.67)	1.00 (0.701)	0.994 (0.999)	0.998 (0.743)	0.997 (0.772)	0.910 (0.816)	0.998 (0.932)	0.999 (0.814)
Refinement								
Reflections used in refinement	64808	32918	92153	54665	54765	24596	26590	21743
Reflections used for R-free	3474	1775	4841	2974	2734	1372	1280	1024
R-work/	0.156	0.156	0.162	0.170	0.172	0.164	0.174	0.166
R-free	0.173	0.190	0.180	0.194	0.180	0.199	0.204	0.203
No of atoms	2629	2792	2722	2503	2619	2664	2331	2579
protein	2328	2487	2337	2257	2367	2424	2215	2400
ligands	22	53	28	36	23	43	13	43
solvent	279	252	357	210	229	197	103	136
RMS deviations								
Bond lengths (Å)	0.014	0.016	0.016	0.014	0.014	0.003	0.009	0.008
Bond angles (°)	1.3	1.29	1.5	1.34	1.32	0.56	1.05	1
Ramachandran								
Favored (%)	98.2	97.0	98.2	98.2	97.9	97.6	96.4	97.3
Allowed (%)	1.4	2.7	1.4	1.4	1.4	2.0	2.9	2.4
Outliers (%)	0.36	0.34	0.36	0.36	0.71	0.34	0.72	0.34
Clashscore	3.42	3.18	5.32	3.11	4	3.28	3.88	2.07
B-factors								
Average B-factor	26.2	33.5	25.6	22.7	22.4	38.2	32.7	27.7
Macro-molecules	25.0	32.32	23.69	22.24	21.82	37.74	32.63	27.57
ligands	41.4	41.67	41.75	21.7	30.18	43.62	48.93	32.26
solvent	34.6	43.11	36.66	27.4	27.35	43.12	31.43	28.4

Table S3: $PTP1B_{L204A}$ residues: specific intermediate exchange group

k_{ex} (s^{-1})	pB (%)	Residues
3000 ± 40	3.4 ± 0.2	I19, I23, V49($C\gamma_2$), I57, I72, V107($C\gamma_1$), L110($C\delta_1$), V113($C\gamma_1$), L119($C\delta_1$&$C\delta_2$), I134, I149, L163($C\delta_1$&$C\delta_2$), I171, V184($C\gamma_1$), L195($C\delta_1$&$C\delta_2$), V212($C\gamma_2$), V213($C\gamma_1$), I219, L227($C\delta_1$&$C\delta_2$), L233($C\delta_1$&$C\delta_2$), I246, V249($C\gamma_2$), L250($C\delta_1$), L251($C\delta_2$), L260($C\delta_1$), I261, L267($C\delta_1$), L272($C\delta_1$), I275
5000 ± 210	0.9 ± 0.1	L140($C\delta_1$&$C\delta_2$), L142($C\delta_1$&$C\delta_2$), L144($C\delta_1$), I281, L294($C\delta_1$)

Table S4: $PTP1B_{L204A}$ residues in complex with TCS401; specific intermediate exchange group

k_{ex} (s^{-1})	pB (%)	Residues
3130 ± 280	0.3 ± 0.1	I19, L140($C\delta_1$&$C\delta_2$), L142($C\delta_1$&$C\delta_2$), L144 ($C\delta_1$ &$C\delta_2$), L294($C\delta_1$)
1340 ± 120	1.9 ± 0.9	L83($C\delta_1$), L110($C\delta_1$), V155($C\gamma_1$), I171, L192($C\delta_1$), L195($C\delta_1$), V211($C\gamma_1$), V213($C\gamma_1$), L227($C\delta_2$), V244($C\gamma_1$&$C\gamma_2$) L250($C\delta_1$), L272($C\delta_1$), I275
680 ± 40	11 ± 1	V49($C\gamma_1$), V107($C\gamma_1$), V113($C\gamma_1$), L119($C\delta_1$), V184($C\gamma_1$), I261

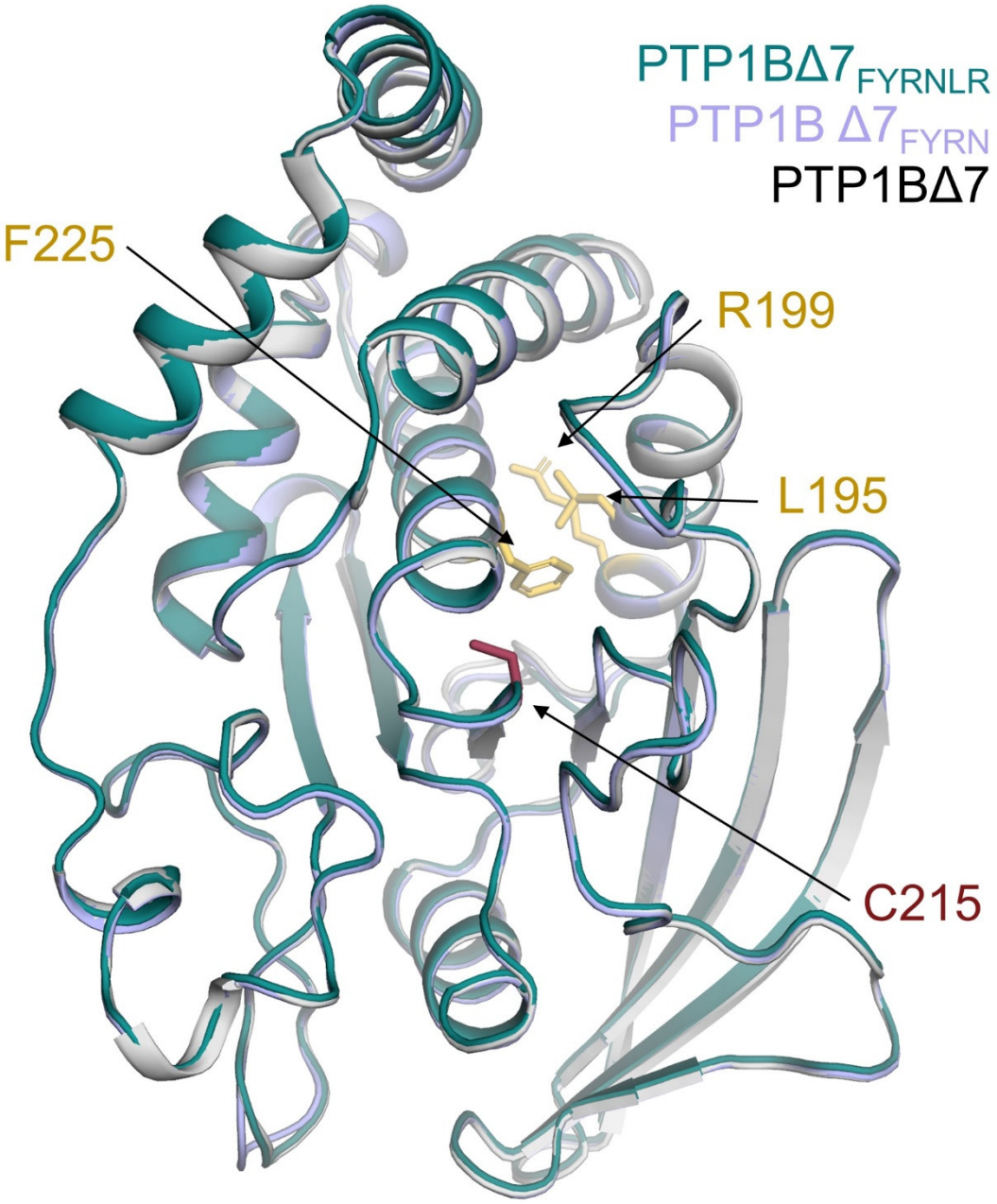

Figure S1. Crystal structures of PTP1BΔ7$_{FYRN}$ and PTP1BΔ7$_{FYRNLR}$. Cartoon overlay of PTP1BΔ7 (PDB 5KA0, grey) with PTP1BΔ7$_{FYRN}$ (PBD 7MN9, light blue) and PTP1BΔ7$_{FYRNLR}$ (PBD 7MOU, teal). Residues mutated in a subset of variants are shown as yellow sticks; catalytic cysteine shown as red stick.

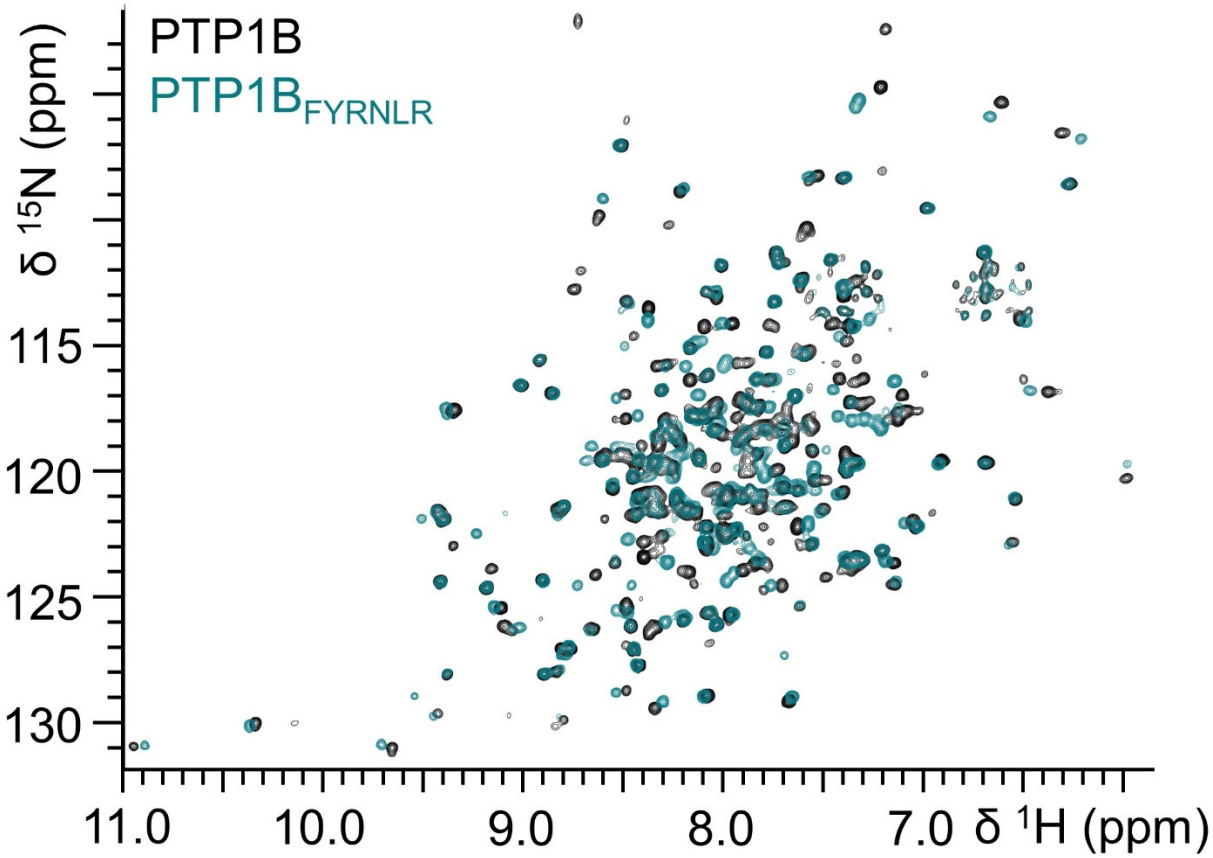

Figure S2. PTP1B$_{FYRNLR}$ NMR spectroscopy data. Overlay of the 2D [^{1}H,^{15}N] TROSY spectrum of PTP1B (black) and PTP1B$_{FYRNLR}$ (teal).

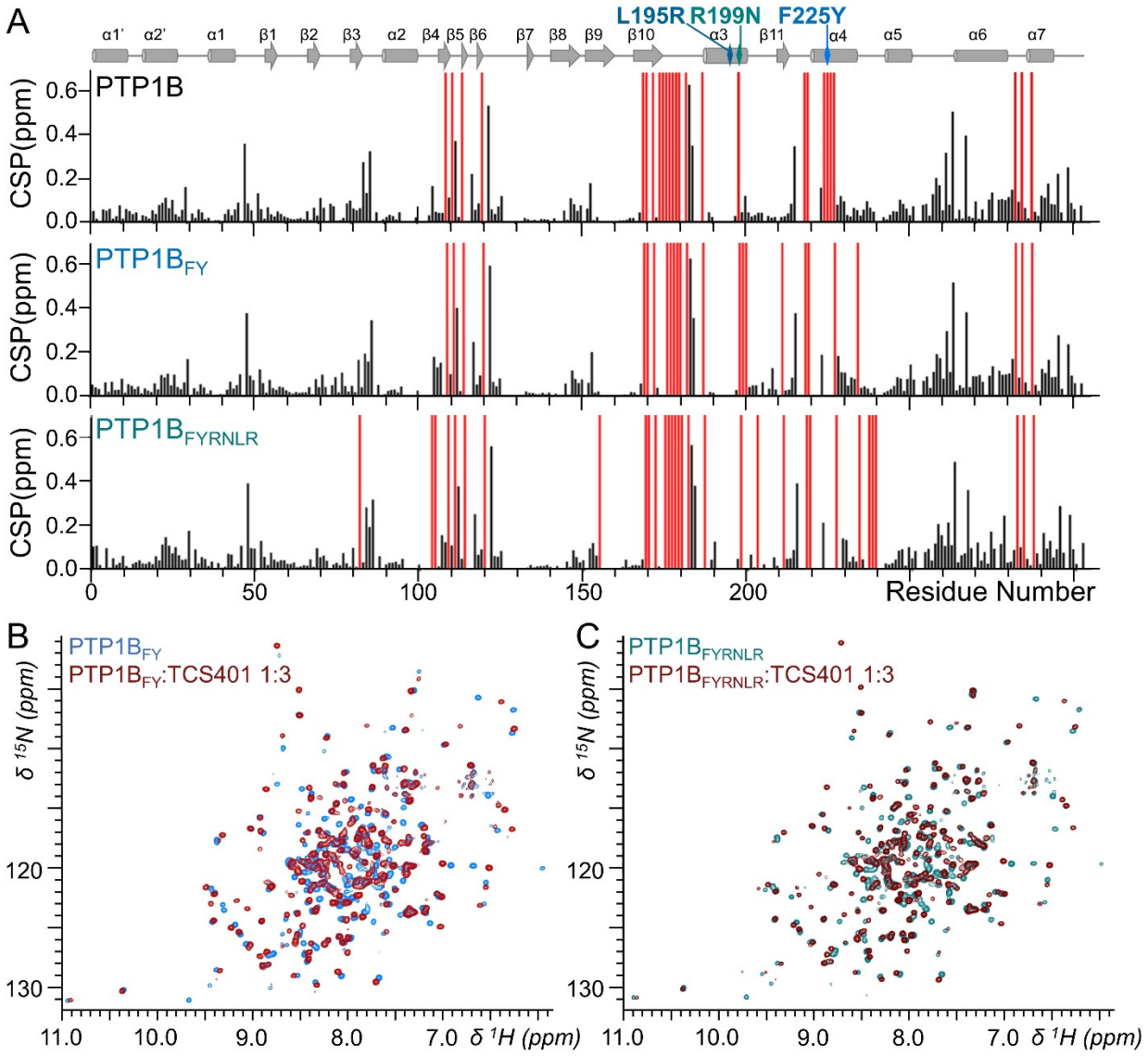

Figure S3. CSP analysis of PTP1B$_{FY}$ and PTP1B$_{FYRNLR}$ vs TCS401. (**A**) CSP vs residue plots of PTP1B, PTP1B$_{FY}$ and PTP1B$_{FYRNLR}$ upon saturation with TCS401. Red bars indicate peaks that broaden beyond detection. PTP1B secondary structural elements are shown above, with the position of mutations indicated by diamonds. (**B**) Overlay of the 2D [^{1}H,^{15}N] TROSY spectra of PTP1B$_{FY}$ (blue) and PTP1B$_{FY}$:TCS401 (red; 1:3 ratio). (**C**) Overlay of the 2D [^{1}H,^{15}N] TROSY spectra of PTP1B$_{FYRNLR}$ (teal) and PTP1B$_{FYRNLR}$:TCS401 (red; 1:3 ratio).

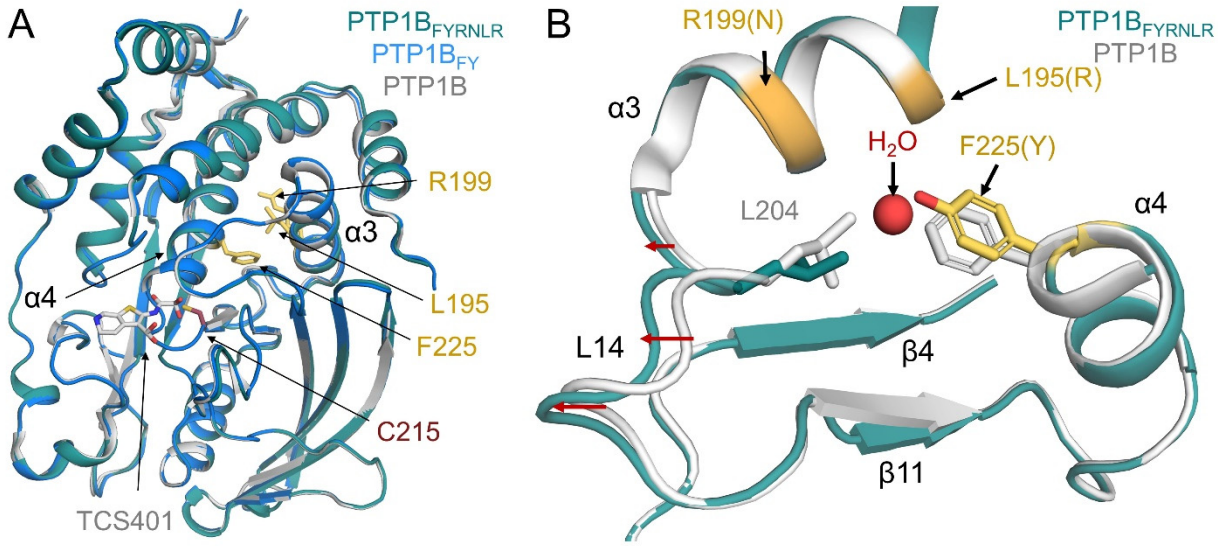

Figure S4: Crystal structures of PTP1B$_{FY}$ and PTP1B$_{FYRNLR}$. (**A**) Cartoon overlay of PTP1B (PDB 5K9VW; grey), PTP1B$_{FY}$ (PDB 7MKZ, blue) and PTP1B$_{FYRNLR}$ (PDB 7MNB, teal). (**B**) Close-up view of structural changes around F225; key residues shown as sticks.

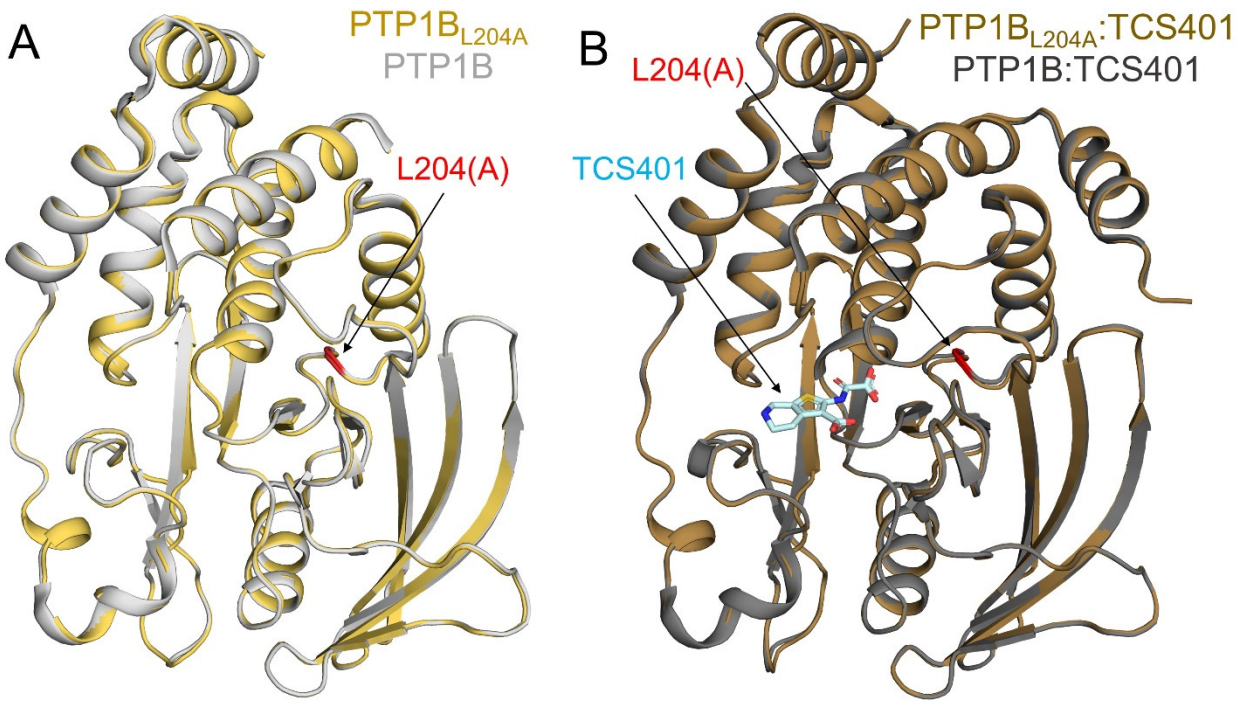

Figure S5: Crystal structure of PTP1B$_{L204A}$. (**A**) Cartoon overlay of PTP1B (PDB 5K9V; grey) and PTP1B$_{L204A}$ (PDB 7MNC, yellow) in the ligand free state. (**B**) Cartoon overlay of PTP1B (PDB 5K9W; dark grey) and PTP1B$_{L204A}$ (PDB 7MND, dark yellow) in complex with TCS401.

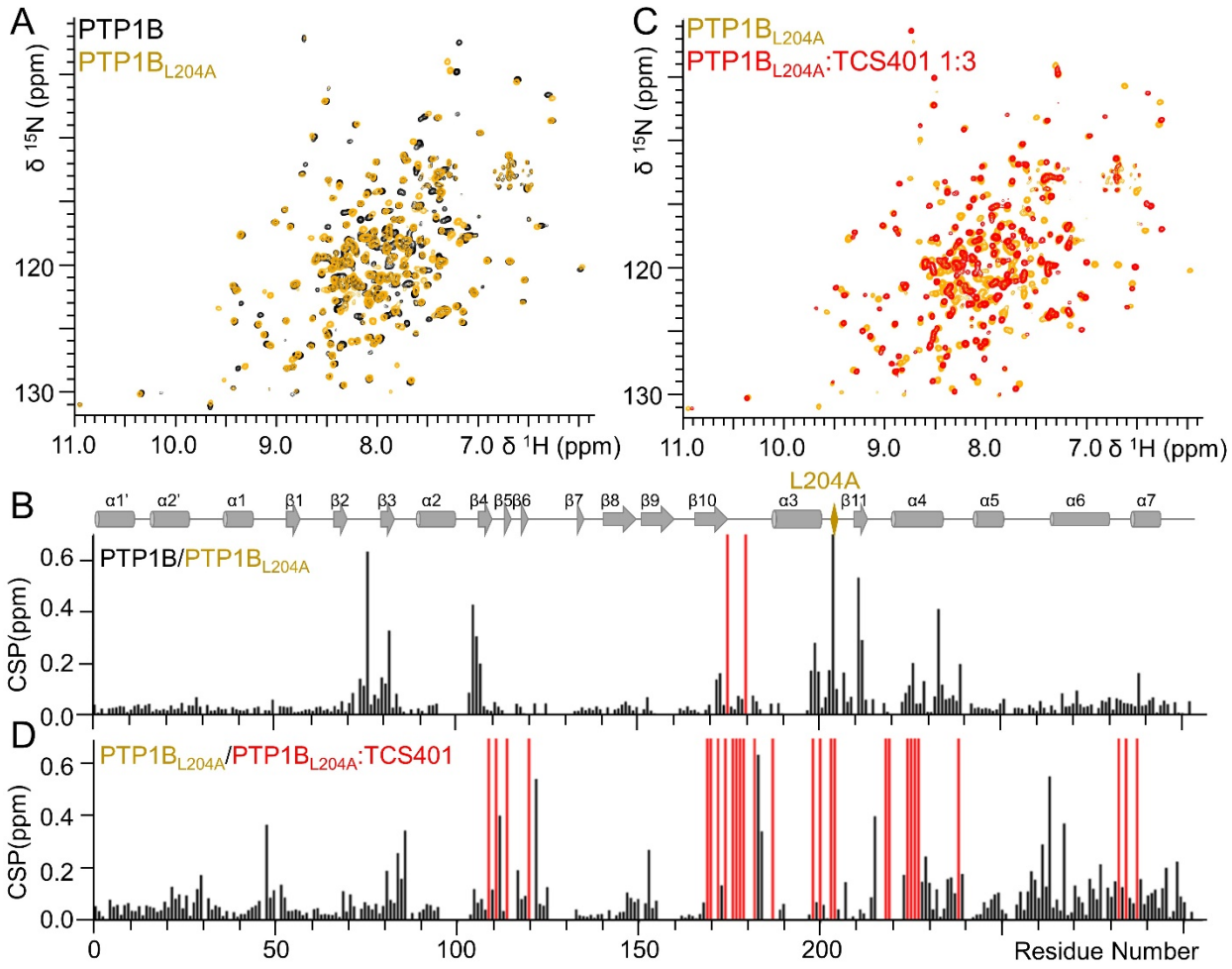

Figure S6. Analysis of the PTP1B$_{L204A}$ TCS401 interaction. (**A**) Overlay of the 2D [^{1}H,^{15}N] TROSY spectrum of PTP1B (black) and PTP1B$_{L204A}$ (yellow). (**B**) CSP vs residue plot of PTP1B and PTP1B$_{L204A}$. Red bars indicate peaks that broadened beyond detection. PTP1B secondary structural elements are shown above with L204A mutation indicated by yellow diamond. (**C**) Overlay of the 2D [^{1}H,^{15}N] TROSY spectrum of PTP1B$_{LA}$ (yellow) with PTP1B$_{L204A}$:TCS401 (red; 1:3 ratio). (**D**) CSP vs residue plot of PTP1B$_{L204A}$ upon saturation with TCS401 (1:3 ratio). Red bars indicate peaks that broadened beyond detection. PTP1B secondary structural elements are shown above with L204A mutation indicated by yellow diamond.

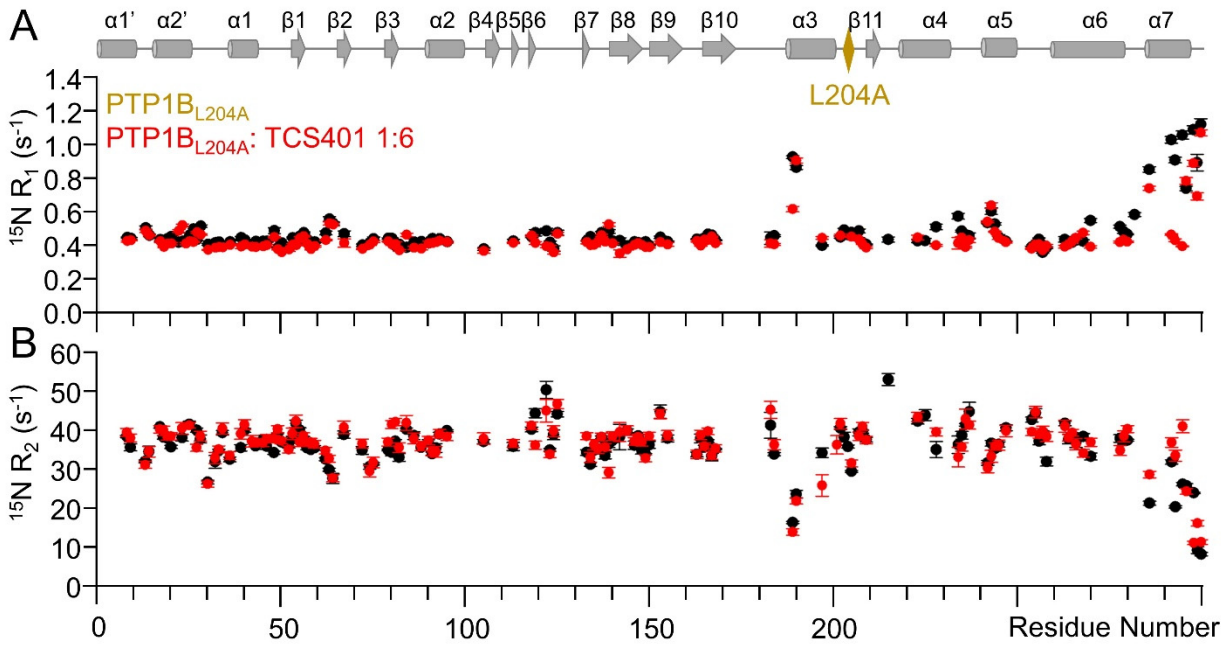

Figure S7. PTP1B$_{L204A}$ ^{15}N fast timescale relaxation data. (**A**) 18.8 T (800 MHz ^{1}H Larmor) R_1 ^{15}N relaxation data for PTP1B$_{L204A}$ (black) and PTP1B$_{L204A}$:TCS401 (1:6 ratio; red) plotted against PTP1B sequence; PTP1B secondary structural elements shown above. L204A mutation indicated by yellow diamond. (**B**) R_2 ^{15}N backbone relaxation data for PTP1B$_{L204A}$ (black) and PTP1B$_{L204A}$:TCS401 (1:6 ratio; red) plotted against PTP1B sequence.

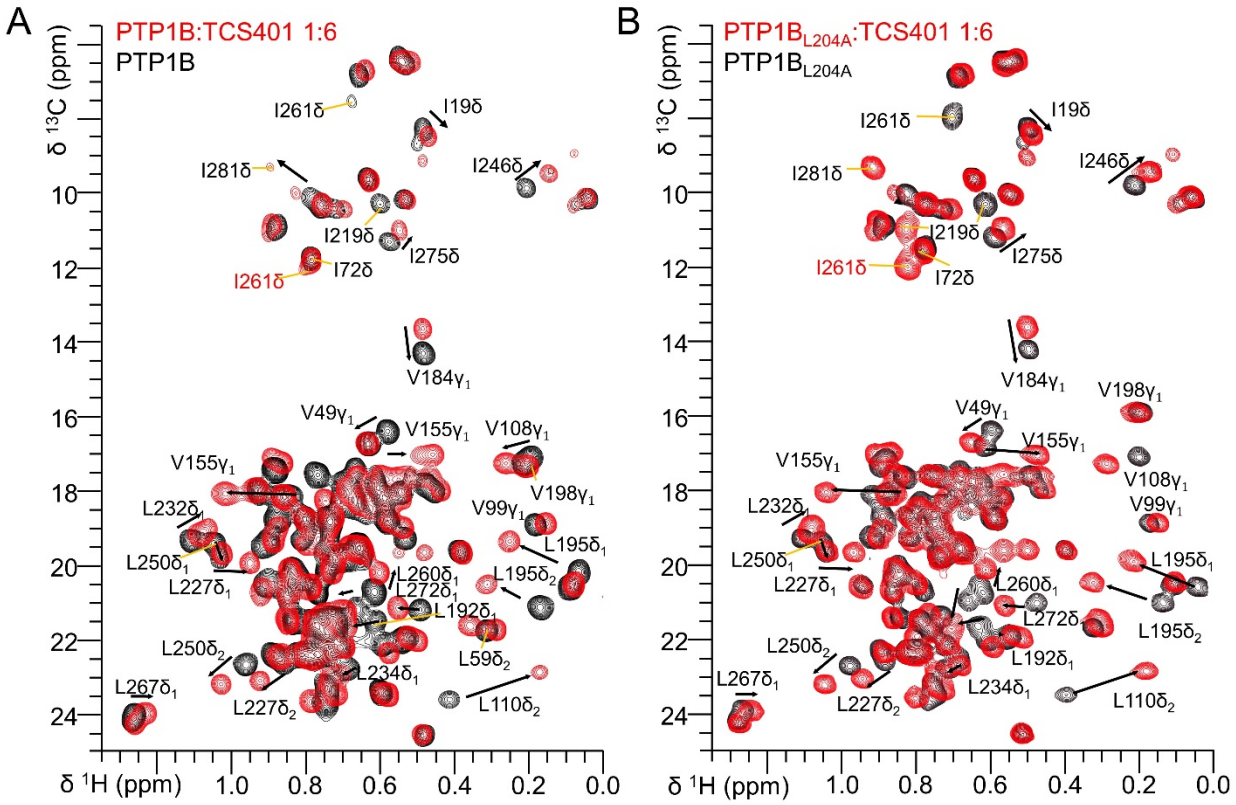

Figure S8. ^{13}C ILV 2D [^{1}H,^{13}C] HSQC spectrum of PTP1B and PTP1B$_{L204A}$ saturated with TCS401. (**A**) Overlayed ^{13}C ILV 2D [^{1}H,^{13}C] HSQC spectrum of PTP1B (black) and PTP1B saturated with TCS401 (1:6 ratio, red). Moving peaks are annotated and indicated with arrows. (**B**) Overlayed ^{13}C ILV 2D [^{1}H,^{13}C] HSQC spectrum of PTP1$_{L204A}$ (black) and PTP1B$_{L204A}$ saturated with TCS401 (1:6 ratio, red). Moving peaks are annotated and indicated with arrows.

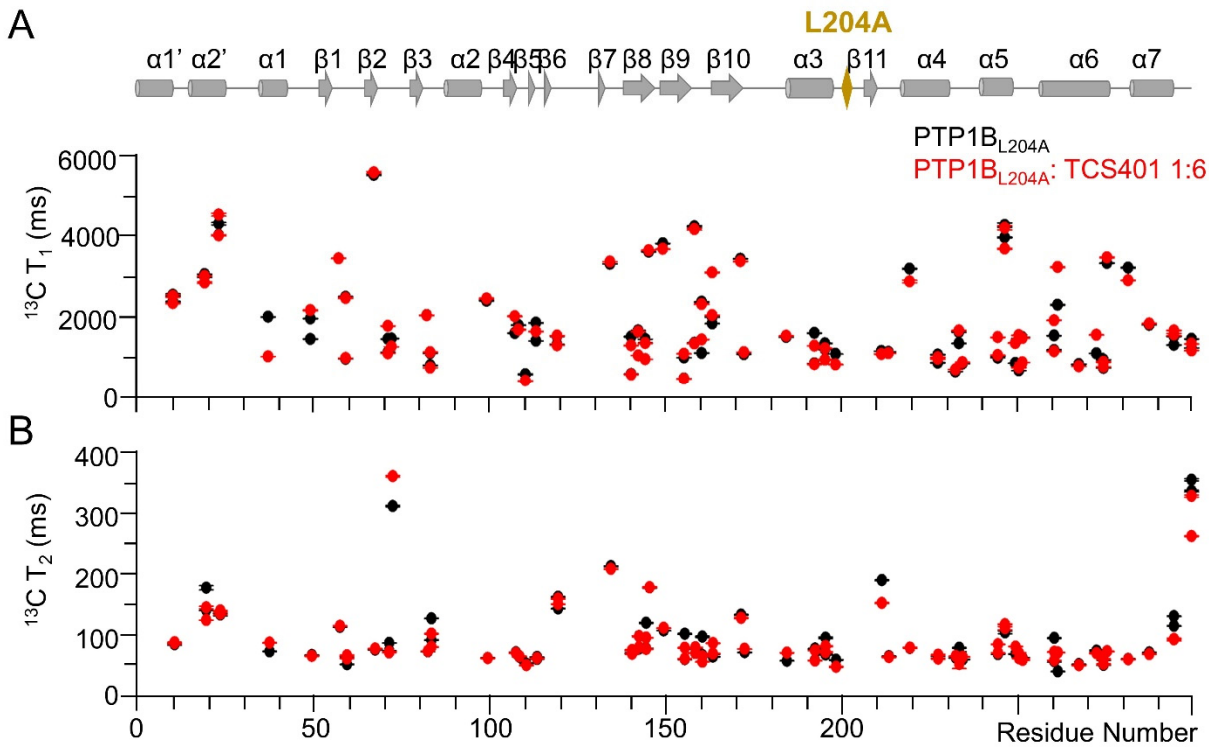

Figure S9. PTP1B$_{L204A}$ ^{13}C ILV fast timescale relaxation data. (**A**) 18.8 T T$_1$ ^{13}C ILV relaxation data PTP1B$_{L204A}$ (black) and PTP1B$_{L204A}$:TCS401 (1:6 ratio; red) plotted against PTP1B sequence; PTP1B secondary structural elements shown above**.** L204A mutation indicated by yellow diamond. (**B**) T$_2$ ^{13}C ILV relaxation data for PTP1B$_{L204A}$ (black) and PTP1B$_{L204A}$:TCS401 (1:6 ratio; red) plotted against PTP1B sequence.

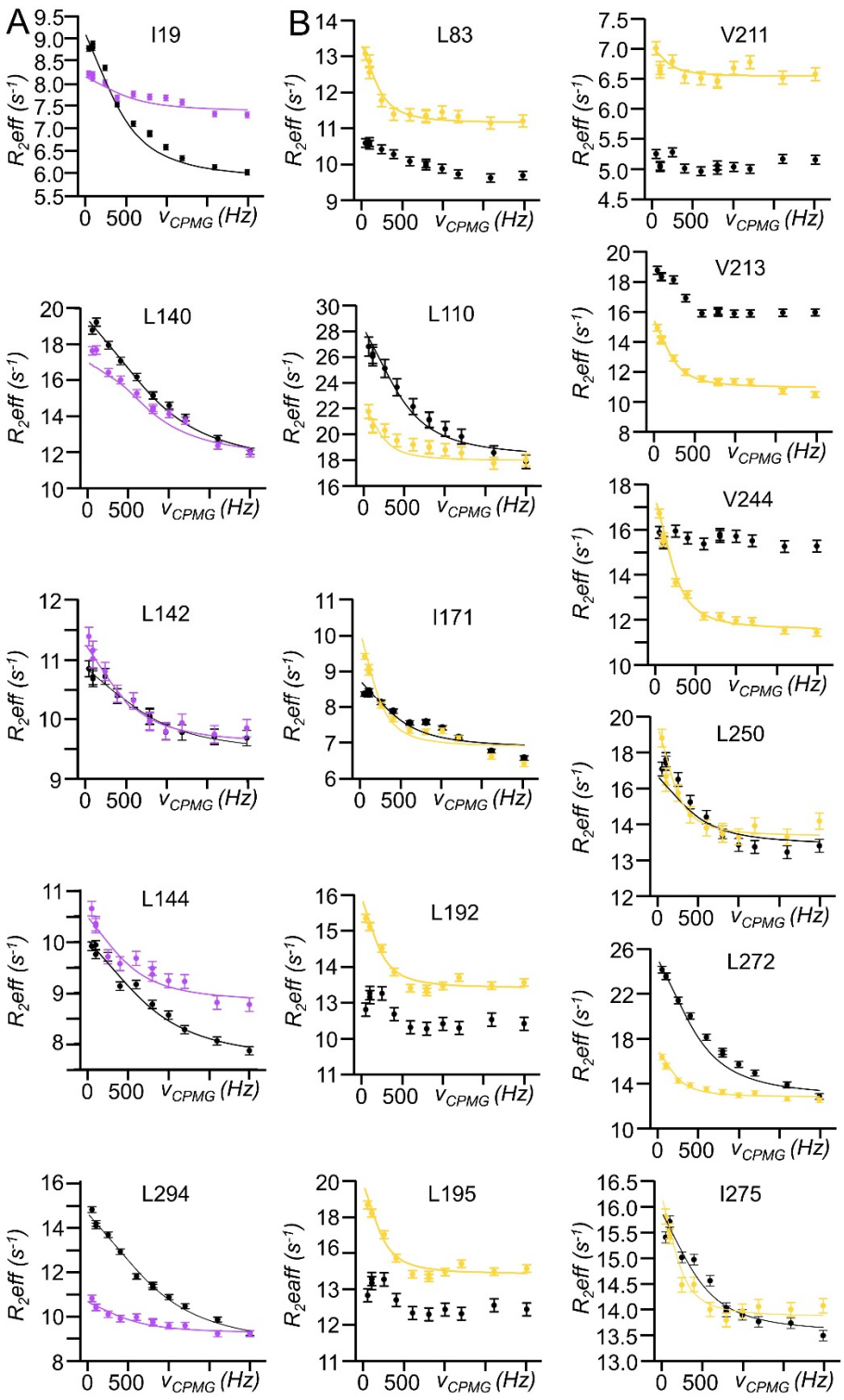

Figure S10. Intermediate timescale ^{13}C ILV relaxation dispersion dynamics of PTP1B$_{L204A}$ upon TCS401 binding. (**A**) Examples of group 1 residues in PTP1B$_{L204A}$ (black) and PTP1B$_{L204A}$:TCS401 saturated (purple). (**B**) Examples of group 2 residues for PTP1B$_{L204A}$ (black) and PTP1B$_{L204A}$:TCS401 saturated (yellow).

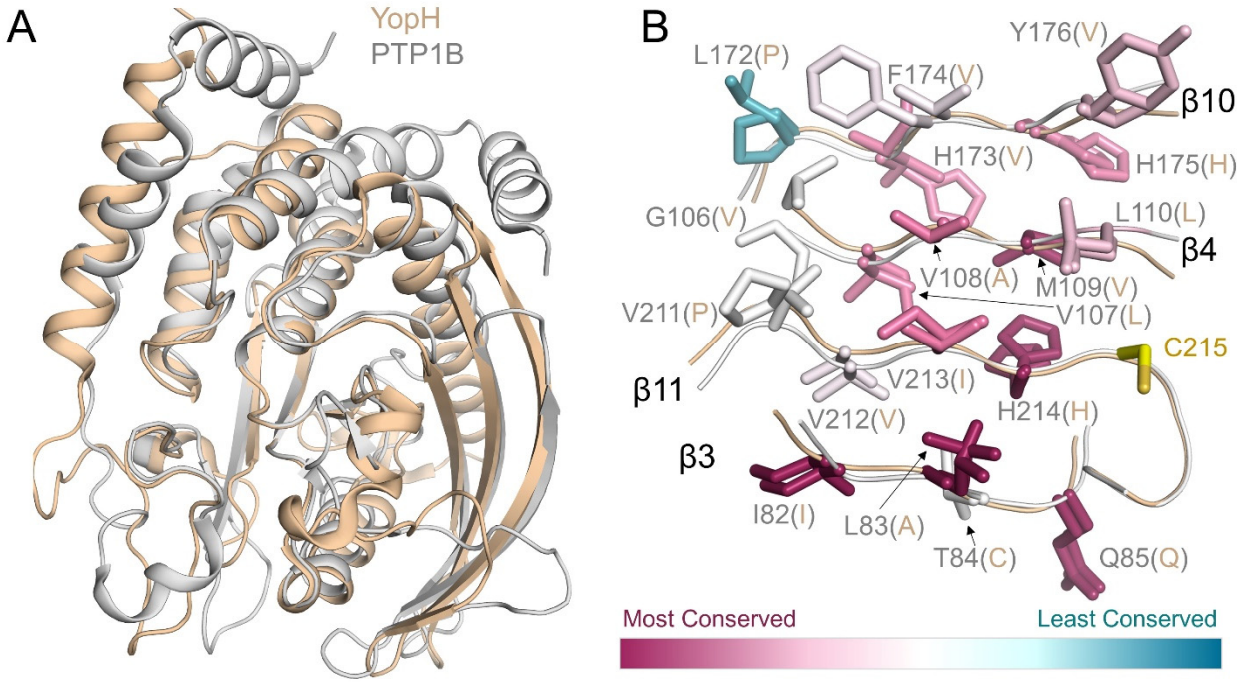

Figure S11. PTP1B and YopH. (**A**) Overlay of PTP1B (PDB 5K9W, gray) with YopH (PDB 1LYV, wheat). (**B**) Overlay of the β-strands β3/β4/β10/β11 with conserved residues shown as sticks.